Oxide Ion Conductivity in $Ln_5Mo_3O_{16+x}$ (Ln = La, Pr, Nd, Sm, Gd; $x \sim 0.5$) with a Fluorite-Related Structure

M. Tsai and M. Greenblatt*

Department of Chemistry, Rutgers, The State University of New Jersey, New Brunswick, New Jersey 08903

W. H. McCarroll

Department of Chemistry, Rider College, PO Box 6400, Lawrenceville, New Jersey 08648

Received October 17, 1988

High oxide ion conductivity has been observed in the $Ln_5Mo_3O_{16+x}$ system with Ln = La, Pr, Nd, Sm, and Gd, $x \sim 0.5$, by ac complex impedance methods in the temperature range 250–700 °C. The $Ln_5Mo_3O_{16+x}$ phases form in a fluorite-related cubic structure. The oxygen content varies in the range $0 \leq x \leq 0.5$. In the reduced phases ($Ln_5Mo_3O_{16+x}$, $x \simeq 0$) the conductivity is dominated by electron hopping due to mixed valent Mo^{5+}/Mo^{6+} and is several orders of magnitude higher than the conductivity of the fully oxidized phases ($Ln_5Mo_3O_{16.5-y}$, $y \simeq 0.0$). The conductivity in $Ln_5Mo_3O_{16.5-y}$ ($y \sim 0$) is ascribed to the motion of O^{2-} ions in the fluorite-related lattice, where some of the empty cavities are partially occupied by the excess ($x \sim 0.5$) oxide ions. The highest oxide ion conductivity was found in $La_5Mo_3O_{16.5-y}$ ranging from 10^{-6} $(\Omega\ cm)^{-1}$ at 275 °C to $\sim 10^{-2}$ $(\Omega\ cm)^{-1}$ at 670 °C with $E_a \simeq 0.84$ eV. The transition from the reduced ($Ln_5Mo_3O_{16}$) to the oxidized ($Ln_5Mo_3O_{16.5}$) phases and the reverse reactions were studied by powder X-ray diffraction, ac impedance, electron spin resonance and differential thermal analysis/thermogravimetric analysis measurements. The conductivity is highly sensitive to oxygen content.

Introduction

Solid oxide electrolytes with significant oxygen anion mobilities are of practical interest because of their applications in such devices as high-temperature fuel cells,[1] O_2 and/or H_2O sensors,[2,3] and oxygen pumps.[4] Among the most prominent examples of such materials are those binary oxides of zirconium, hafnium, cerium, and thorium that have been doped with relatively large amounts of alkaline-earth or trivalent rare-earth oxides. All have fluorite or fluorite-related structures that are deficient in oxygen and have high oxygen mobilities. In the case of yttrium-stabilized zirconia, ionic conductivities of the order of 10^{-1} $(\Omega\ cm)^{-1}$ have been reported in the 1000 °C region.[5]

There exist a number of relatively poorly characterized ternary oxides of molybdenum with the rare-earth metals that contain molybdenum in both the penta- and hexavalent states. They have been variously formulated as $Ln_3Mo_2O_{10}$, $Ln_5Mo_3O_{16}$, $Ln_7Mo_4O_{22}$, and $Ln_{12}Mo_6O_{35}$.[6-14] Of these, only the $Ln_5Mo_3O_{16}$ where Ln = La, Ce, Pr, Nd, or Sm appear well established. Hubert,[10] who first identified these compounds on the basis of their X-ray powder diffraction patterns, concluded that they were most probably isomorphous with $CdTm_4Mo_3O_{16}$.[15] Evidence that these compounds might more properly be formulated as $Ln_5Mo_3O_{16+x}$ where $0 \leq x \leq 0.5$ was implied by Hubert, who reported that $La_5Mo_3O_{16}$ and $Nd_5Mo_3O_{16}$ could be heated in air above 300 °C without loss of structure and that the process resulted in color changes and a slight increase in the cubic lattice constant.[10,13] The proposed structure of this compound on the basis of X-ray powder diffraction data[15] was more fully elucidated by a single-crystal X-ray diffraction study of the $CdY_4Mo_3O_{16}$ isomorph by Bourdet et al. in 1981.[16] They showed that the cations occupy the metal positions of a doubled fluorite unit cell in a partially ordered fashion while the oxygens are displaced from their ideal positions to form a distorted tetrahedral environment for molybdenum. In contrast, the cadmium and yttrium atoms retain a near-cubic coordination (Figure 1). McCarroll et al. were able to prepare small single crystals of both $La_5Mo_3O_{16+x}$ and $Nd_5Mo_3O_{16+x}$ by fused salt electrolysis at 1050–1100 °C.[17] The crystals grow as small dark green cubes at the cathode, and their Ln:Mo ratios were confirmed by chemical analysis. Although the value of x is small, it is clearly greater than zero for reasons that will be discussed. Preliminary work in our laboratories showed that these crystals could be oxidized by heating in air at 500 °C to yield a yellow phase (La) or a pink phase in the case of Nd and that their single-crystal nature was not lost. Further, they could be partially reduced, as evidenced by color changes, by heating in hydrogen at temperatures as low as 150 °C. In addition, their electrical resistivities (qualitative two probe) increased from about 10^5 Ω cm to a value in excess of 10^7 Ω cm upon oxidation.

These properties suggested that significant ionic conductivity might exist in this type of phase at moderately elevated temperatures. The results of our conductivity studies are presented here along with additional data that

(1) Rohr, F. J. *Application of Solid Electrolytes*; Takahashi, T., Kozawa, A., Eds.; JEC Press: Cleveland, 1980; p 196.
(2) Worrell, W. L. *Solid Electrolytes*; Geller, S., Ed.; Springer-Verlag: Berlin, 1977; p 163.
(3) Goto, K. S. *Solid State Electrochemistry and its Applications to Sensors and Electronic Devices*; Elsevier: Amsterdam, 1988; p 333.
(4) Naito, K.; Tsuji, T.; Watanabe, S. *Solid State Ionics* **1980**, 509.
(5) Steele, B. C. H.; Drennau, J.; Slotwinski, R. K.; Bonanos, N.; Butler, E. P. Advances in Ceramics, *Science and Technology of Zirconia*, Eds. Heuer, A. H., Hobbs, L. W., Eds.; American Ceramics Society: Columbus, 1981; Vol. 3, p 286.
(6) Hubert, P. H. *Compt. Rend. Ser. C* **1967**, *264*, 1600.
(7) Hubert, P. H. *Compt. Rend. Ser. C* **1969**, *269*, 1287.
(8) Hubert, P. H. *Compt. Rend. Ser. C* **1970**, *271*, 1179.
(9) Restituito, F.; Faurie, J. P. *Compt. Rend. Ser. C* **1973**, *276*, 783.
(10) Hubert, P. H.; Michel, P.; Thozet, A. *Comp. Rend. Ser. C* **1973**, *276*, 1779.
(11) Hubert, P. H. *Bull. Soc. Chim. Fr.* **1975**, 475.
(12) Restituito, F.; Faurie, J. P. *Rev. Chim. Miner.* **1974**, *11*, 97.
(13) Hubert, P. H. *Bull. Soc. Chim. Fr.* **1976**, 1755.
(14) Hubert, P. H. *Compt. Rend. Ser. C* **1974**, *279*, 405.
(15) Faurie, J. P.; Kohlmuller, R. *Rev. Chim. Miner.* **1971**, *8*, 241.
(16) Bourdet, J. B.; Chevalier, R.; Fournier, J. P.; Kohlmuller, R.; Omaly, J. *Acta Crystallogr.* **1982**, *B38*, 2371.
(17) McCarroll, W. H.; Jakubicki, G.; Darling, C. *J. Solid State Chem.* **1983**, *48*, 189.

0897-4756/89/2801-0253$01.50/0

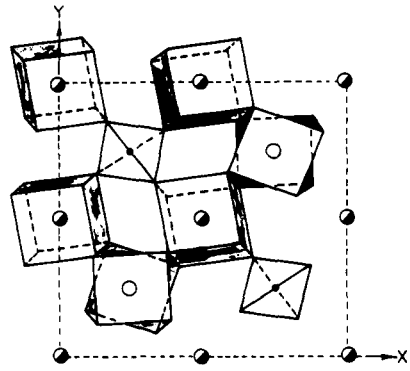

Figure 1. Crystal structure of $CdY_4Mo_3O_{16}$ (after ref 16).

more clearly defines the range of oxygen stoichiometry in these phases.

Experimental Section

All samples were prepared by solid-state reactions using stoichiometric amounts of the appropriate rare-earth oxides, MoO_2 and MoO_3, all reagent grade or better. Samples for chemical analysis and initial X-ray studies to define the oxygen stoichiometry were prepared by sealing pellets of the thoroughly ground mixtures in evacuated silica ampules under 50 mTorr of pressure and firing at 1000 °C for 24 h followed by regrinding, repelleting, and refiring at 1050 °C for an additional 48 h. Portions of some of these samples were oxidized in air at temperatures ranging from 500 to 1200 °C for periods of 6–24 h.

A somewhat different regime was employed for making pelletized samples for conductivity measurements. Nominally stoichiometric quantities of reactant mix were initially heated in vacuo for 20 h at 925 °C and then reground, pelleted, and fired for an additional 16 h at 1000 °C. Both procedures produced single-phase materials as judged from their X-ray powder diffraction patterns. Oxidized samples for conductivity measurements were obtained by heating pellets in air at 550 °C for 10 h. It should be noted that the oxidized phase of the lanthanum compound cannot be prepared by direct reaction of the rare-earth oxide and MoO_3, while the neodymium isotype can.

X-ray powder diffraction patterns were obtained by using either a Philips diffractometer or a Scintag Model PAD V unit. Nickel-filtered copper radiation was used throughout. Cell parameters were obtained by using a least-squares method. Silicon or molybdenum served as internal standards.

Ionic conductivities were measured by an ac complex impedance technique using a Solartron Model 1250 frequency analyzer and 1186 electrochemical interface that were programmed by a Hewlett Packard 9816 desktop computer for data collection and analysis. Contact to the samples was made by coating the faces of the pellets with either platinum paste or silver paint. A frequency range 10 Hz to 65 kHz was employed by using a heating rate of 200 °C/h over the range 25–700 °C. The resistance due to the electrode–electrolyte polarization effect appeared to be small and was considered to be insignificant for the oxidized samples. Reduced samples were measured in a nitrogen atmosphere, while the oxidized samples were measured in air. The conductivity changes that occur upon oxidation were observed by heating the reduced phases in air. Since the reduced $Ln_5Mo_3O_{16+x}$ phases with $x \simeq 0$ are slowly oxidized on standing in air even at room temperature, all such samples were stored either in evacuated sealed ampules or in a helium-filled drybox until ready for use.

Thermogravimetric analysis (TGA) and differential thermal analysis (DTA) measurements were carried out by using a Du Pont Model 9900 thermal analyzer, and electron spin resonance spectra (ESR) were obtained with a Varian spectrometer. Chemical analyses for total rare-earth and molybdenum content as well as the average oxidation number of molybdenum were determined by standard wet chemical methods that have been described elsewhere.[17]

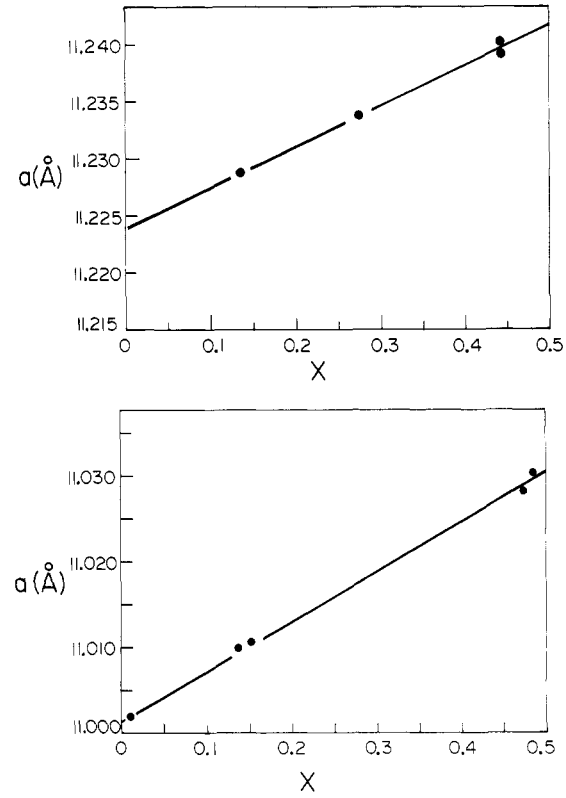

Figure 2. Variation of the experimentally determined values of the lattice parameters with the value of x in $La_5Mo_3O_{16+x}$ (top) and $Nd_5Mo_3O_{16+x}$ (bottom).

Table I. Correlations in Weight Gain, Unit Cell Parameter a_0, and Mo(V) Content upon Oxidation of $Ln_5Mo_3O_{16}$ (Ln = La, Nd)[a]

sample	Mo(V) (obsd), %	x (obsd)	a_0	% wt gain obsd	% wt gain calcd
La–1	5.65	0.135	11.2287 (5)		
La–2	0.84	0.445	11.2393 (5)	0.62	0.62
Nd–1	7.45	0.012	11.0019 (4)		
Nd–2	0.22	0.486	11.0303 (4)	0.62	0.60

[a] Correlation of weight gains observed upon oxidation with those calculated on the basis of lattice constant and percent Mo(V). Samples labeled –2 were prepared by heating samples labeled –1 in air at 550 °C for 6 h.

Results and Discussion

Oxygen Stoichiometry. A notable feature of the $Ln_5Mo_3O_{16+x}$ phases is their variable oxygen content. A convenient measure of x is easily obtained by the measurement of the cubic lattice constant since there is a linear relationship between x and a_0. This is shown in Figure 2 for the La (top) and Nd (bottom) systems, where the value of x, based upon percent Mo(V), was determined titrametrically. In both cases the extrapolation of the curve to $x = 0$ yields a value of the lattice constant that is close to the lowest value that we have observed for freshly prepared, reduced samples. The slopes of the curves are also consistent with the weight gain upon oxidation that was observed for some samples as shown in Table I. This provides an independent measure for the validity of the curves.

The meaning of the extrapolated value of a_0 for $x = 0.50$, i.e., complete oxidation, is less certain. For the La system this value is 11.2415 Å. In this respect we note that we

Table II. Cell Parameters of $Ln_5Mo_3O_{16+x}$[a] as a Function of Ln(III) Radius

	Ln				
	La	Pr	Nd	Sm	Gd
Ln(III) radius,[b] Å	1.30	1.27	1.25	1.22	1.19
red. lattice, Å	11.2238 (6)	11.0737 (5)	11.0020 (1)	10.8981 (4)	10.8080 (1)
ox. lattice, Å	11.2400 (2)	11.1007 (3)	11.0304 (4)	10.9277 (2)	10.8384 (3)
lattice expan, Å	0.0162	0.0270	0.0284	0.0296	0.0304
Hubert data,[c] Å	11.215	11.050	10.995	10.890	10.800

[a] $x = 0$ for the reduced phases; $x \simeq 0.5$ for the oxidized phases. [b] Effective radii for 8 CN Ln(III). [c] See ref 10.

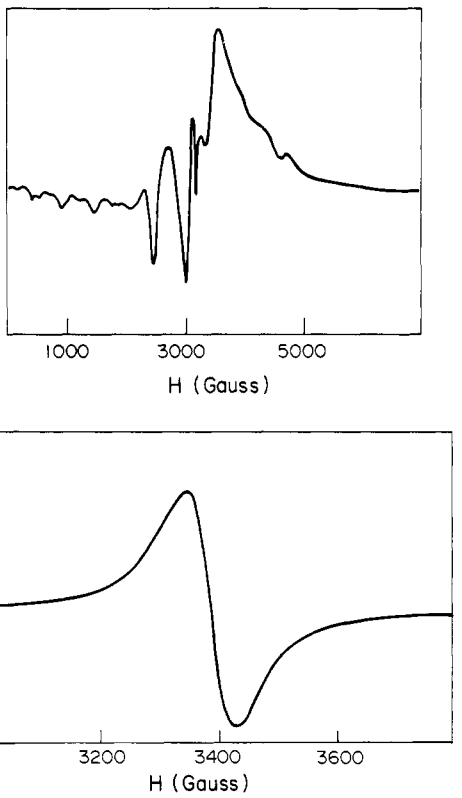

Figure 3. Electron spin resonance spectrum of $La_5Mo_3O_{16+x}$ ($x \simeq 0.5$) (top) and $La_5Mo_3O_{16}$ (bottom).

have never observed a value of a_0 higher than 11.2405 (5) Å for polycrystalline samples prepared by solid-state reactions (Table II). However values as high as 11.2445 (5) Å have been obtained from pulverized samples of single-crystal material, prepared by fused salt electrolysis and heated at 800 °C for several hours. These discrepancies could be related to oxygen ordering effects that may take place as x approaches 0.50. Similar effects are noted in the neodymium system.

It should also be noted that materials approaching the composition $La_5Mo_3O_{16.5}$ cannot be prepared by a solid-state reaction of constituent binary oxides; rather, the reduced phase must be prepared first and then oxidized. Further it is unlikely that the fully oxidized lanthanum phase exists. Heating of a sample, previously oxidized at 600 °C in air, at 1000 °C for 4 h results in a partial loss of color and decomposition into a mixture of La_2MoO_6 and $La_2Mo_2O_9$ as evidenced by new lines in the X-ray powder diffraction pattern. The decomposition is largely complete after an additional 28 h of heating, with La_2MoO_6 now being the dominant phase. Moreover, the sample is now very nearly colorless. This is consistent with the reaction

$$2La_5Mo_3O_{16.5-y} + yO_2 \rightarrow 4La_2MoO_6 + La_2Mo_2O_9$$

Further evidence, apart from chemical analysis, that Mo(V) is still present in the yellow lanthanum phase prepared by oxidation between 500 and 700 °C is given by

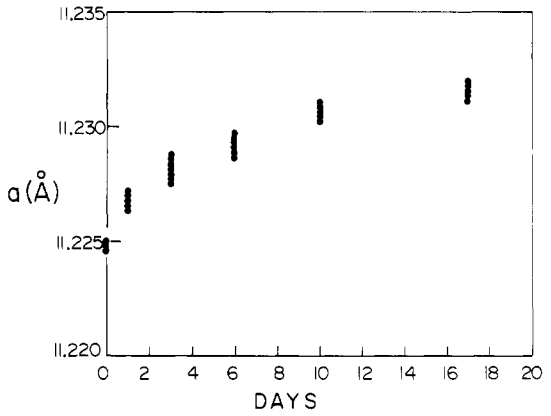

Figure 4. Variation of the lattice constant of $La_5Mo_3O_{16}$ as a function of time at ambient room temperature.

the ESR spectrum shown in Figure 3, top. This spectrum shows three rather sharp ESR peaks (~100–200 G wide, each) at around $g \sim 1.90$. The peaks are attributed to a small concentration of Mo(V) centers in different crystallographic sites. The small resonances, particularly sharp on the left side of the main peaks, are hyperfine peaks associated with the nuclear spin of $I = {}^5/_2$ of the ^{95}Mo and ^{97}Mo isotopes of molybdenum. The gyromagnetic ratios of these two isotopes are nearly equal; thus the hyperfine structure arising due to both of these isotopes will overlap. When the yellow sample of $La_5Mo_3O_{16.5-y}$ is heated in air at 1225 °C for 24 h, the signal seen in Figure 3, top, is nearly completely absent in the ESR. Indeed, at 1225 °C Mo(V) is not expected to be stable in air. In contrast, the ESR spectrum of a dark green reduced sample of $La_5Mo_3O_{16+x}$ shows a single, very broad (~1000 G wide) peak at $g \sim 1.90$ without any resolution of the hyperfine structure (Figure 3, bottom). The line broadening is ascribed to spin–spin interactions of a large concentration of Mo(V) centers in the reduced phase.

On the other hand, the oxidized form of the neodymium compound can be prepared by direct reaction of Nd_2O_3 and MoO_3. Here the value of x, as shown by chemical analysis, appears to be very close to the stoichiometric value provided the final oxidation temperature does not exceed approximately 1000 °C. Limited exploratory experiments above that temperature show that the samples *lose* weight (0.1–0.3%), indicating possible loss of MoO_3, while no significant changes in the X-ray powder diffraction patterns are noted. Further investigation would be of value.

The reduced phases $Ln_5Mo_3O_{16+x}$ with $x \sim 0$ are dark green, while the oxidized phases with x approaching 0.5 are yellow (Ln = La, Sm, Gd) or light green in sunlight but pink under a tungsten lamp (Ln = Nd, Pr). The reduced phases are quite air sensitive. Figure 4 shows a plot of the lattice constant vs time for a sample of $La_5Mo_3O_{16}$ that was allowed to stand in room ambiance for several days. The oxygen uptake after 11 days corresponds to a value of $x = 0.207$. The rate of oxygen uptake appears to be influenced by the presence of water since we have noted that in a more humid (albeit uncontrolled) labora-

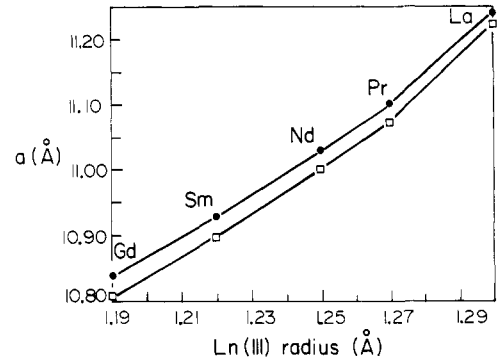

Figure 5. Variation of the lattice parameters of the reduced (□) and oxidized (●) phases of $Ln_5Mo_3O_{16+x}$ as a function of Ln(III) effective ionic radii.

tory environment, a sample of $La_5Mo_3O_{16+x}$ with initial value of $x = 0.005$ had reached $x = 0.277$ in the 8-day period after the ampule was opened, based upon lattice constant changes. Single-crystal specimens prepared by fused salt electrolysis in general oxidize much more slowly, but even here there seems to be some sample dependency.

Powder X-ray diffraction patterns show that both the reduced and the fully oxidized compounds studied here are single phase with *Pn3n* cubic symmetry. The lattice parameters of the reduced phases are slightly larger than those reported by Hubert et al.[10,18] (Table II). The lattice parameters of both the fully oxidized and reduced phases decrease with decreasing effective Ln(III) radii (Figure 5, Table II). The magnitude of lattice expansion from the reduced $Ln_5Mo_3O_{16}$ to the fully oxidized $Ln_5Mo_3O_{16+x}$ (except for Ln = La) is substantial as shown in Table II. It seems that the smaller the radius of Ln(III), the greater the lattice expansion. This suggests that in the $Ln_5Mo_3O_{16+x}$ phases, the electrostatic repulsions between the inserted oxygen ions and the oxide ion sublattice increase as the lattice shrinks. The anomalously low value of a_0 for the oxidized La phase arises in part from the fact that some Mo(V) is necessary to stabilize the lattice as discussed above.

Ac Complex Impedance Measurements. Restituito and Faurie studied the conductivity of $Ce_5Mo_3O_{16}$ and found it to be a p-type semiconductor.[12] Hubert, on the other hand, reported n-type semiconducting behavior for $La_5Mo_3O_{16}$.[11] Our measurements on both single-crystal and polycrystalline specimens of $Ln_5Mo_3O_{16+x}$ ($x \sim 0$) indicate n-type behavior. This is attributed to the mixed valency of $Mo^{5+/6+}$, which can lead to electronic conductivity via an electron-hopping mechanism. Indeed, it is expected that the electron states of molybdenum will be highly localized for the $CdY_4Mo_3O_{16}$ structure since the MoO_4 tetrahedra are discrete (see Figure 1). In this respect Torardi has, by single-crystal X-ray diffraction analysis, confirmed that $La_5Mo_3O_{16}$ is isomorphous with $CdY_4Mo_3O_{16}$.[19] A similar study of an $La_5Mo_3O_{16.5}$ crystal was unable to locate the additional oxygen with certainty, leading to the conclusion that it must be distributed statistically in a number of interstitial sites.

From ac complex impedance measurements of $La_5Mo_3O_{16}$ the bulk conductivities of the sample have been determined both in air and N_2 in the temperature range 25–700 °C. Figure 6, curve 1, shows the temperature variation of conductivity of $La_5Mo_3O_{16}$ in air from 25 to

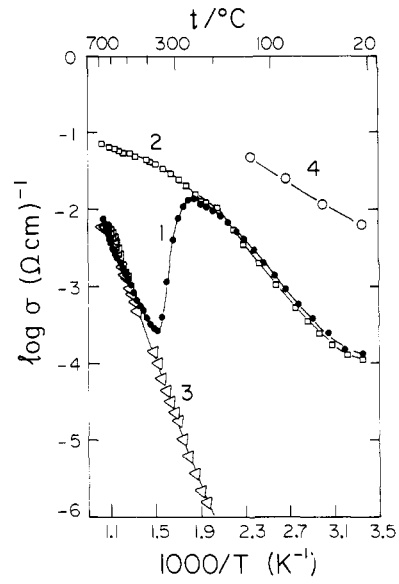

Figure 6. Arrhenius plots of the total conductivity of ●, $La_5Mo_3O_{16}$ (reduced phase) heated in air; ○, $La_5Mo_3O_{16}$ (reduced phase) heated in He/5% H_2 atmosphere; □, $La_5Mo_3O_{16}$ (reduced phase) heated in N_2 atmosphere; △, $La_5Mo_3O_{16.5-y}$ (oxidized phase) heated in air.

700 °C. From room temperature to ~267 °C the conductivity is modestly high ($\sim 10^{-4}$–10^{-2} $(\Omega\ cm)^{-1}$) and increases with increasing temperature. At ~267 °C a sharp decrease in the conductivity is seen. At ~383 °C the conductivity increases sharply again with increasing temperature. The region 25–267 °C is attributed primarily to electronic conductivity (i.e., electronic conductivity, σ_e, is orders of magnitude greater than the ionic conductivity, σ_i) and corresponds to semiconducting behavior, due to electron hopping from Mo^{5+} to Mo^{6+} as discussed above. The decrease in the conductivity in the temperature range ~267–383 °C is ascribed to oxygen uptake and concomitant loss of electron carriers with increasing O^{2-} content as Mo^{5+} is oxidized to Mo^{6+} (i.e., $La_5Mo_3O_{16+x}$, $x > 0$). The dramatic increase in the conductivity of a sample of $La_5Mo_3O_{16+x}$ heated in air (Figure 6, curve 1) beyond ~383 °C is ascribed to oxide ion motion which now dominates the conductivity process.

To probe the nature of conductivity in $La_5Mo_3O_{16+x}$ reduced phases, we measured the conductivity of $La_5Mo_3O_{16}$ in N_2 atmosphere in a separate series of complex impedance measurements. Results of this investigation shown in Figure 6, curve 2, indicate that the log σ vs $1000/T$ data of $La_5Mo_3O_{16}$ measured in air and those measured in N_2 completely overlap in the temperature range 25–267 °C. However, in contrast to the sample that is heated in air (curve 1), the conductivity in N_2 (curve 2) continues to increase with rising temperature beyond 267 °C. The presence of a well-defined semicircle in the ac complex impedance of this sample even in the low-temperature regime (25–267 °C) was attributed to electrode polarization effects due to the reaction $^1/_2O_2(g) + 2e^- \rightarrow O^{2-}$ (electrolyte) taking place at the interface.[20] The source of oxygen may be the Pt electrode surface, which tends to adsorb O_2 from the surrounding air, and/or the nitrogen atmosphere (contaminated with O_2) used for the measurement. Indeed, after the sample and the Pt electrodes were heated up to 600 °C in a He/5% H_2 reducing atmosphere, the electrode polarization reaction was elimi-

(18) Hubert[13,14] suggests that the reduced Gd analogue actually has the composition $Gd_7Mo_4O_{22}$ based on the presence of very weak lines in his X-ray pattern. Since we see no new lines in our samples with the $Gd_5Mo_3O_{16}$ stoichiometry, we will continue to use this formula in this paper.
(19) Torardi, C., unpublished research, private communication.

(20) Raistrick, I. D.; McDonald, J. R.; Franceschetti, D. R. *Impedance Spectroscopy*; McDonald, J. R., Ed.; Wiley: New York, 1987; p 25.

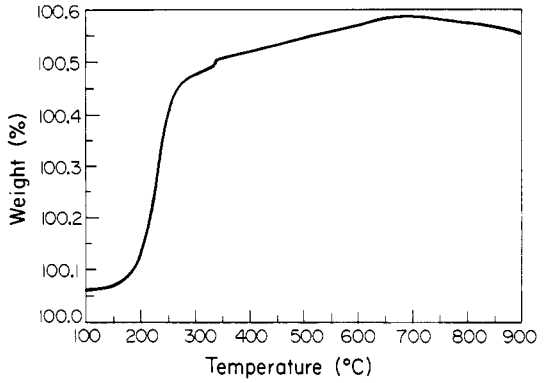

Figure 7. Thermogravimetric analysis (TGA) of $La_5Mo_3O_{16}$ measured in air.

nated as evidenced by the absence of the semicircle in the ac complex impedance measurement. The conductivity data of $La_5Mo_3O_{16}$ measured in He/5% H_2 atmosphere coincides with curve 4 in Figure 6.

From analysis of the ac complex impedance data and simple equivalent circuit modeling, we obtained the resistance due to polarization: If this is subtracted from the total resistance of the sample to yield the electronic conductivity of the reduced phases, values consistent with those of curve 4, Figure 6, are obtained. The corrected conductivities are (curve 4, Figure 6), about 2 orders of magnitude greater, which implies that the real decrease in the conductivity from electronic to ionic conductivity is much greater than the 2 orders of magnitude indicated by curve 1 Figure 6.

We have also carried out four probe dc measurements of conductivity on nearly fully reduced $La_5Mo_3O_{16}$ sample in an N_2 atmosphere; the ac and dc results are nearly identical. This is another piece of confirming evidence that the conductivity is primarily electronic in the nearly reduced samples.

Curve 3 of Figure 6 shows the temperature variation of conductivity for nearly fully oxidized $La_5Mo_3O_{16.5-y}$ ($y \sim 0$) sample measured in air. In the temperature range ~ 383–700 °C, these data completely overlap with curve 1. In $La_5Mo_3O_{16.5-y}$ nearly all of the molybdenums are in the 6+ oxidation state. The conductivity of this sample is several orders of magnitude lower than that of the reduced $La_5Mo_3O_{16}$ phase throughout the temperature range 25–700 °C. Moreover, differential thermal analysis (DTA) of a sample of reduced $La_5Mo_3O_{16}$ shows an exothermic transition at ~240 °C, indicating oxygen uptake, close to the anomaly observed (~267 °C) in the conductivity data. Similarly, thermogravimetric analysis (TGA) of a sample of $La_5Mo_5O_{16}$ in air shows a sharp increase in weight at ~220 °C (Figure 7). All of these results support the great ease of diffusion of O^{2-} in $Ln_5Mo_3O_{16+x}$ phases and that fast oxide (O^{2-}) ion motion in the lattice dominates the conductivity for $Ln_5Mo_3O_{16.5-y}$ ($y \sim 0$). Similar behavior of the temperature variation of the conductivity as seen in Figure 6 is observed for all the rare-earth $Ln_5Mo_3O_{16+x}$ (Ln = Pr, Nd, Sm, and Gd) compounds. The temperature where oxygen uptake commences in the reduced phases was determined from DTA/TGA (T_{ox}) and ac impedance (T_{ei}) measurements (Table III). Both T_{ox} and T_{ei} increase with decreasing Ln(III) radii. This may again be attributed to increasing electrostatic repulsions between the inserted oxygens and oxygen sublattice as the $Ln_5Mo_3O_{16+x}$ lattice shrinks. T_{ei} is always significantly higher than T_{ox}, because a critical concentration of O^{2-} content is required (or a critical decrease in the concentration of Mo^{5+}/Mo^{6+}) before the conductivity ascribed to electronic motion drops dramatically in the impedance measurement.

Table III. Transition Temperatures (°C) from the Reduced ($Ln_5Mo_3O_{16}$) to the Oxidized Phases ($Ln_5Mo_3O_{16.5}$)

	Ln				
	La	Pr	Nd	Sm	Gd
T_{ox}[a]	240	245	250	255	304
T_{ei}[b]	267	272	277	305	370

[a] T_{ox}, obtained by DTA/TGA analysis, is the oxidation transition temperature from reduced phase to oxidized phase. [b] T_{ei}, obtained by ac impedance measurement, is the transition temperature from electronic conductivity to ionic conductivity (i.e., the temperature where a sharp drop in the conductivity of the reduced phases measured in air is observed).

Table IV. Activation Energies of Electronic (in $Ln_5Mo_3O_{16}$ Phases) and Ionic (in $Ln_5Mo_3O_{16.5}$ Phases) Conductivities

	Ln				
	La	Pr	Nd	Sm	Gd
electronic					
E_a,[a] eV	0.25 (1)		0.23 (1)		0.21 (1)
ionic					
E_a,[b] eV	0.81	0.72	0.69	0.60	0.59
E_a*, eV	0.84	0.85	0.86	0.92	1.04
log A, $(\Omega\ cm)^{-1}$; high T	2.33	2.02	1.77	1.79	2.35
log A, $(\Omega\ cm)^{-1}$; low T	2.07	1.10	0.55	−0.37	−0.56

[a] E_a for the electronic conductivity was obtained from measurement of ac conductivity of the reduced phases ($x = 0$) in nitrogen from 25 to 700 °C. Correction for electrode polarization was made (e.g., curve 4, Figure 6). [b] Ionic conductivity parameters of activation energies and A were obtained from measurement of ac conductivity of the oxidized phases ($x = 0.5$) in air from 250 to 700 °C.

The electronic activation energy (E_a) of the semiconducting regime (curve 1 and 2, Figure 6; 24–267 °C) decreases with decreasing Ln(III) radius (Table IV). This might be due to polarization effects. The highest electronic conductivities (without polarization effect) are $\sim 10^{-1}$ $(\Omega\ cm)^{-1}$ at ~700 °C and are about the same order of magnitude in all of the rare-earth compounds investigated. Interestingly, the electronic conductivity of reduced $Ln_5Mo_3O_{16}$ phases (i.e., Figure 6, curve 2) measured in N_2 atmosphere appears to saturate at high temperature (~700 °C).

A further study of the ionic conductivity as a function of oxygen content was carried out by heating/cooling a sample of $Nd_5Mo_3O_{16.5-y}$ in a nitrogen atmosphere and in air. $Nd_5Mo_3O_{16+x}$ appears to be the most stable compound in the series. Figure 8, curve 1, corresponds to the conductivity of a sample of $Nd_5Mo_3O_{16.5-y}$ heated in N_2 atmosphere; curve 2 is the cooling path of curve 1 in N_2. Curve 3 corresponds to heating the sample in air, after the cooling cycle in N_2 gas. Curve 4 is the cooling path of curve 3 in air. $Nd_5Mo_3O_{16.5-y}$ lost part of its oxygen content when heated in N_2 atmosphere, and the electronic conductivity becomes significant. This is indicated by the higher conductivity seen in curve 2 compared to curve 1 due to mixed electronic and ionic conductivity. This is supported by TGA results as well, which show a small weight loss of the samples occurring in N_2 atmosphere above 300 °C. Curve 3 shows a transition temperature due to the oxidation reaction similar to the behavior observed in Figure 6, curve 1. Thus the oxygen lost by the heat treatment under N_2 is regained upon heating in air. The oxygen content of the sample corresponding to curve 3 at high T is probably higher than that corresponding to curve 1 at corresponding temperatures. The sample of curve 4 has even lower conductivity than that corresponding to curve 3 due to some oxygen loss when heating to high temperature even in air. However, when the sample of curve 3 is cooled in air, it is expected to regain oxygen and curves 3 and 4

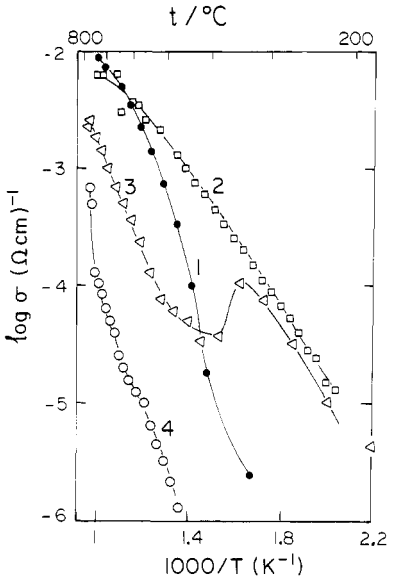

Figure 8. Arrhenius plots of the ionic conductivity of $Nd_5Mo_3O_{16+x}$ ($0 < x < 0.5$). The same sample was cycled in heating and cooling according to the following regimen: ●, nearly fully oxidized phase heated in N_2 gas; □, cooled in N_2 gas; △, heated in air; ○, cooled in air.

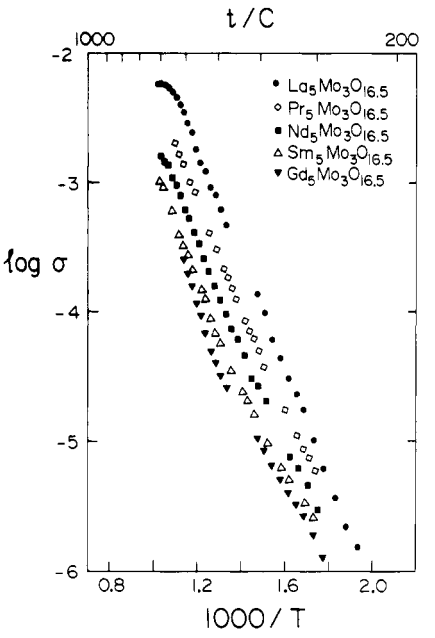

Figure 9. Arrhenius plots for nearly completely oxidized $Ln_5Mo_3O_{16.5}$, Ln = La, Pr, Nd, Sm, and Gd.

might be expected to overlap. These discrepancies in the data may be due to the fact that the samples are not at equilibrium. The results shown in Figure 8 demonstrate that the conductivity of $Nd_5Mo_3O_{16+x}$ is extremely sensitive to small changes in oxygen content, a property that might be exploited for application as an oxygen sensor.

The temperature variation of ionic conductivity measured in air on the nearly fully oxidized $Ln_5Mo_3O_{16.5-y}$ (Ln = La, Pr, Nd, Sm, and Gd) are shown in Figure 9. Clear breaks in the slopes of these log σ vs $1000/T$ curves suggest that different mechanisms of conductivity are extant in the low- and high-temperature regions (the low-temperature region for the La compound is not included in Figure 9). We have used the expression $\sigma = A \exp(-E_a/RT)$ to calculate ionic activation energies (E_a) and preexponential factors A. These values are summarized in Table IV. As the Ln(III) radius decreases, the high-temperature activation energy (E_a*) increases and the low-temperature activation energy (E_a) decreases. Overall however, Figure 9 shows that the ionic conductivity increases with increasing Ln(III) radius. The highest conductivity was found to be $\sim 10^{-2}$ $(\Omega\ cm)^{-1}$ at 670 °C in $La_5Mo_3O_{16.5-y}$ with E_a* (high T) = 0.84 eV (Figure 9). The preexponential factors are all of the same order of magnitude, suggesting that the disorder of the anion sublattice is similar in all of the isostructural $Ln_5Mo_3O_{16.5}$ compounds.

Given the reversible nature of the low-temperature oxidation–reduction properties of these compounds, which occur without loss of basic structure, we believe that the primary conduction process involves mobile interstitial oxide ions. An important contributor to the activation energy in this region will be the energy required to allow the oxide ion to move through narrow cation orifices from one interstice to another. A second factor will be the attractive energy between the molybdenum which has undergone oxidation and the inserted oxygen. At higher temperatures the formation of vacancies in the regular oxygen sublattice may be important. This may account for the decrease in the activation energy at high temperatures. The deviation from Arrhenius behavior seen for $La_5Mo_3O_{16.5-y}$ in Figure 9 may be due to some type of saturation effect. A dynamic steady-state concentration of vacancies and mobile ions might be formed above this temperature. Similar behavior was seen in the Nd sample, and Figure 9 also suggests a tapering off of the conductivity at high temperature for the Sm analogue as well.

There is also the possibility of a significant number of oxygen lattice vacancies being formed in the oxygen sublattice at low temperatures which result in the formation of complex, defect clusters consisting of the oxidized molybdenum (analogous to an aliovalent dopant cation), induced lattice vacancies, and the interstitial oxide ions. Such clusters are well established in anion-excess fluorides with fluorite-related structures.[21-24] Although we find no X-ray diffraction evidence for such clustering, it would be very difficult to detect, because of the relatively low "doping" level, which corresponds to less than 1% of the electron density of the unit cell. However, such interactions could have a significant, deleterious effect upon oxide ion migration.

It is expected that as the size of the rare-earth cation increases, the radius of the orifice between interstices will decrease. This is in line with the trend observed for the low-temperature activation energy (E_a). On the other hand, Kilner and Brook have pointed out that increasing the polarizability of the host cation in fluorite type oxides lowers the migration energy of the oxide ion.[25] In this respect it is noteworthy that the ionic conductivities in this series of compounds do follow this trend (Figure 9).

At high temperatures, activation energies increase with decreasing rare-earth metal size. While this does follow the cation polarizability trend, we also note that the La compound is not as thermally stable as the Nd compound, a trend that should conform with the ease of formation of defects. On the other hand, we note that the Gd compound is less stable than the Nd compound, which runs counter to the trend. It would appear therefore that the

(21) Cheetham, A. K.; Fender, B. E. F.; Cooper, M. J. *J. Phys. C* **1971**, *4*, 3107.
(22) Catlow, C. R. A.; Chadwick, A. V.; Corish, J. *J. Solid State Chem.* **1983**, *48*, 65.
(23) Laval, J. P.; Frit, B. *J. Solid State Chem.* **1983**, *49*, 237.
(24) Laval, J. P.; Mikow, A.; Frit, B.; Pannetier, *J. Solid State Chem.* **1986**, *61*, 359.
(25) Kilner, J. A.; Brook, R. J. *Solid State Ionics* **1982**, *6*, 237.

mechanism of conductivity is quite complex and that further study will be required to understand and optimize the conductivity process.

Although monotonic trends are observed in the activation energies (Table IV), we note that within each set the values are similar, suggesting that the conduction mechanism is the same in all compounds, which in turn suggests, in line with Kilner and Brook's arguments,[25] that the nature of the crystal structure is the dominant factor in determining migration energies.

In summary, high oxide ion conductivity has been observed for $Ln_5Mo_3O_{16.5-y}$ (Ln = Nd, Pr, Sm, and Gd) which have a fluorite-related structure. The highest ionic conductivity was found in $La_5Mo_3O_{16.5-y}$ ranging from 10^{-6} at 275 °C to about 10^{-2} $(\Omega\ cm)^{-1}$ at 670 °C. Yttrium-stabilized zirconias show oxide ion conductivities of about the same order of magnitude in this temperature range. However, the variable oxygen stoichiometry of the $Ln_5Mo_3O_{16+x}$ phases and the sensitivity of the ionic conductivity to oxygen content suggests that these materials might prove to be good oxygen sensors.

Acknowledgment. We thank Prof. John Sheats of Rider College and Prof. Charles Dismukes of Princeton University for the ESR measurements and Dr. S. Tanase, Visiting Research Scientist from GERIO, Japan, for useful discussions. This work was supported by the ONR (M.T. and M.G.) and the National Science Foundation's Research in Undergraduate Institutions (RUI) Program, Solid State Chemistry Grant DMR-88-42788 (W.H.McC.).

Polyquinoline-Supported Ruthenium Catalysts: Selective Oxidation of Alcohols with Coated Electrodes

S. J. Stoessel, C. M. Elliott, and J. K. Stille*

Department of Chemistry, Colorado State University, Fort Collins, Colorado 80523

Received October 25, 1988

Two ruthenium complexes containing the novel 2-(2-pyridyl)-4-phenylquinoxaline ligand (qpy), $[Ru(trpy)(qpy)OH_2]^{2+}$ (**11**) and $[Ru(bpy)(qpy)pyOH_2]^{2+}$ (**18**) (trpy = 2,2′,2″-terpyridyl, bpy = 2,2′-bipyridyl, py = pyridine), were prepared as models for complexes supported on polyquinolines (**9**) containing qpy units in the backbone. These polymer complexes, $[Ru(trpy)(polymer\ 9)OH_2]^{+}$ (**13**) and $[Ru(bpy)(polymer\ 9)pyOH_2]^{2+}$ (**20**), were synthesized by a sequence of ligand-replacement reactions on $Ru(trpy)Cl_3$ and $[Ru(bpy)py_4]Cl_2$, respectively. Complexes **11** and **18** were catalytically active for the electrochemical oxidation of secondary alcohols to ketones and allylic or benzylic primary alcohols to aldehydes. Unactivated primary alcohols were not oxidized. Polyquinoline-containing ruthenium complexes **13** and **20** coated on electrodes were more selective and were not catalytically active in the electrochemical oxidation of secondary alcohols (or unactivated primary alcohols), but oxidation of benzylic and allylic alcohols to aldehydes took place. None of the catalysts carried the oxidation further to the corresponding carboxylic acids. Catalytic currents as high as 1 mA were observed.

Ruthenium oxides containing terpyridyl (trpy) and bipyridyl (bpy) ligands, for example, $[Ru(trpy)(bpy)O]^{2+}$ and $[Ru(bpy)_2pyO]^{2+}$, oxidize primary alcohols and allylic and benzylic methyl groups to carboxylic acids; secondary alcohols are oxidized to ketones.[1] These oxides can be generated by the electrochemical oxidation of the corresponding monoaquo complexes $[Ru(trpy)(bpy)OH_2]^{2+}$ (**1**) and $[Ru(bpy)_2pyOH_2]^{2+}$ (**2**). The oxidation reactions of the organic substrates can be effected catalytically with respect to **1** by carrying out the oxidation in a bulk electrolysis cell in which the anode reoxidizes the ruthenium(II) product.

To attach such a ruthenium catalyst to the electrode surface and thereby realize some of the advantages of the modified electrode, a polymer analogue of **2** was developed by coordination of the ruthenium complex to poly(vinylpyridine) (PVP).[2,3] The initial cyclic voltammogram (CV) of this complex, $[Ru(bpy)_2(PVP)OH_2]^{2+}$, on a glassy carbon electrode was similar to the CV of **2**, but after successive scans, the growth of a new wave was apparent at the expense of previous couples, probably as a result of the oxidation of the benzylic carbon on PVP.[1,3]

The utilization of a chemically stable polymer such as a polyquinoline that has no available oxidation sites was therefore of interest in the preparation of ruthenium-modified electrodes. The synthesis of high molecular weight polyquinolines, obtained by the acid-catalyzed condensation of aromatic *o*-amino ketones with aromatic ketomethylene compounds,[4] can be tailored to incorporate a variety of structural features.[5] In the synthesis of such a polymer support, the incorporation of bipyridyl-like ligands in the polymer backbone was of particular interest, since these ligands should mimic the bpy ligand in ruthenium complexes **1** and **2**.

Results and Discussion

Synthesis of a Polyquinoline Support. To ensure that the acid-catalyzed condensation reaction with the 2-acetylpyridine-type ketomethylene monomer would take place and to obtain a model ligand analogous to that

(1) (a) Thompson, M. S.; Giovani, W. F.; Moyer, B. A.; Meyer, T. J. *J. Org. Chem.* **1981**, *49*, 4972. (b) Thompson, M. S.; Meyer, T. J. *J. Am. Chem. Soc.* **1982**, *104*, 5070.
(2) Samuels, G. J.; Meyer, T. J. *J. Am. Chem. Soc.* **1981**, *103*, 307.
(3) Thompson, M.S. Dissertation, University of North Carolina, 1981.
(4) Cheug, C. C.; Yan, S. J. *Org. React.* **1982**, *28*, 37.
(5) Stille, J. K. *Macromolecules* **1981**, *14*, 870.

0897-4756/89/2801-0259$01.50/0